Reduction of Intermodulation Distortion in Microwave Active Bandpass Filters—Theory and Experiments

Kwok-Keung M. Cheng, *Member, IEEE,* and Siu-Chung Chan

***Abstract*—This paper examines, both theoretically and experimentally, the dependency of the third-order intermodulation (IM) distortion and power saturation upon circuit and device parameters of an active bandpass filter using negative-resistance compensation. Nonlinear analysis is performed by means of the Volterra series formulation. We show that the IM distortion can be reduced by several orders of magnitude with suitable choice of external gate–source and feedback capacitance values. Measured performances of some 900-MHz experimental MESFET bandpass filters are presented.**

***Index Terms*—Intermodulation distortion, microwave active filters, Volterra series.**

I. Introduction

NARROW-BAND filters are widely used in microwave systems. Conventionally, these filters have been built as hybrid microwave integrated circuits (MIC's) based upon distributed or lumped components. The development of monolithic-microwave integrated-circuit (MMIC) technology offers the attractive advantages of size reduction and higher functional integration. However, at microwave frequencies, the Q-factor of the on-chip inductors is typically low and, hence, passive narrow-band MMIC filters usually exhibit high insertion loss and poor selectivity. Moreover, the performance of tunable narrow-band MMIC filters is degraded further by the low Q-factor of on-chip varactors. In recent years, the negative-resistance techniques [1]–[3] have been proposed for use in MMIC filters to compensate for component losses, especially of the spiral inductors. These techniques enable the design of microwave active filters with zero insertion loss and excellent channel selectivity. However, due to the inherent nonlinearity of active device, undesirable intermodulation (IM) distortion can be produced when two or more signals are applied to the filter simultaneously. Particularly, the third-order IM distortion has severe effects on the performance of most communication systems. Thus, minimization of IM distortion is often a critical requirement. Recently, a few reports have been published [4] on the study of IM distortion in microwave active filters by computer simulations. Yet, a systematic approach is lacking. In this paper, we show, both theoretically and experimentally, how the intermodulation and power saturation performances of an active bandpass filter using MESFET devices may be optimized. The active filter circuit has been analyzed by the Volterra-series approach [5] and the main formulas are given to indicate how the in-band third-order IM distortion can be reduced by proper circuit design and choice of component values.

Manuscript received June 16, 1998.

The authors are with the Department of Electronic Engineering, The Chinese University of Hong Kong, Shatin, Hong Kong.

Publisher Item Identifier S 0018-9480(00)00851-6.

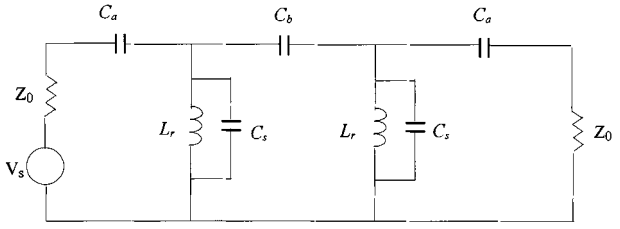

Fig. 1. Lossless lumped-element bandpass filter.

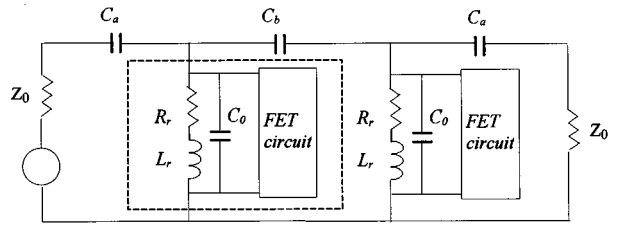

Fig. 2. Lossy filter with negative-resistance compensation.

II. Active Bandpass Filters Using Negative-Resistance Circuits

Among the many active filter topologies, the direct coupling of negative-resistance circuits to a coupled-resonator (LC) filter [1]–[3] has been widely studied due to its simplicity in structure. Without loss of generality, the lumped-element second-order bandpass filter topology [6], shown in Fig. 1, is used in the analyses (for design equations, see the Appendix). Such a configuration is well-suited for MMIC implementation because it does not require large distributed elements. Fig. 2 shows how negative-resistance circuits may be employed to compensate for the inductor losses. The negative-resistance circuit (Fig. 3) basically comprises a MESFET, a feedback capacitor C_f, and an external gate-to-source capacitor C_{ext}. In the figure, $Z_s(\omega)$ represents the circuit impedance of the biasing network, which behaves as an open circuit at high frequencies. The equivalent neg-

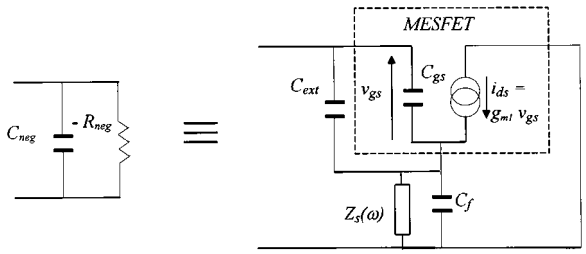

Fig. 3. Equivalent model of the FET circuit.

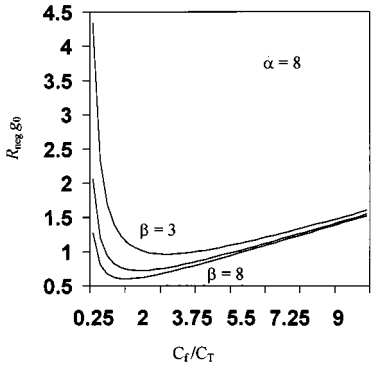

Fig. 4. Variations of $R_{\rm neg}g_0$ versus C_f/C_T and β.

ative resistance and capacitance generated by the FET circuit are given by

$$R_{\rm neg} = \frac{\left(\frac{\alpha}{\beta}\right)^2 + \left(1+\frac{C_f}{C_T}\right)^2}{g_0 \alpha \frac{C_f}{C_T}} \tag{1}$$

$$C_{\rm neg} = \left(1+\frac{C_f}{C_T}\right)\frac{C_T}{\alpha R_{\rm neg} g_0} \tag{2}$$

where

$$\alpha = \frac{g_{m1}}{g_0}$$
$$\beta = \frac{\omega_0 C_T}{g_0}$$
$$C_T = C_{\rm gs} + C_{\rm ext}$$
$$\frac{1}{g_0} = Q^2 R_r$$

and ω_0 is the center frequency of the passband. For illustration, the variations of $R_{\rm neg}g_0$ as a function of C_f/C_T and β (for $\alpha = 8$) is plotted in Fig. 4. Generally speaking, the values of $R_{\rm neg}$ and $C_{\rm neg}$ are both frequency dependent and, thus, this technique is usable only for narrow-band applications. To proceed, the lossy inductor is modeled as a parallel combination of a resistor ($R \approx Q^2 R_r$) and a lossless inductor ($L \approx L_r$), under the assumption that $Q \gg 1$ ($Q = \omega_0 L_r/R_r$). Also, in order to have the exact cancellation of the inductor loss by the negative-resistance circuit, the necessary condition is given as

$$R_{\rm neg} g_0 = 1. \tag{3}$$

As a result, (1) and (2) may be rewritten as

$$\left(1+\frac{C_f}{C_T}\right)^2 + \frac{\alpha^2}{\beta^2} = \alpha\frac{C_f}{C_T} \tag{4}$$

and

$$C_{\rm neg} = \left(1+\frac{C_f}{C_T}\right)\frac{C_T}{\alpha}. \tag{5}$$

The solutions of (4) are given by

$$\frac{C_{f(\pm)}}{C_T} = \frac{\alpha}{2} - 1 \pm \sqrt{\alpha\left(\frac{\alpha}{4}-1\right) - \frac{\alpha^2}{\beta^2}} \tag{6}$$

where $C_{f(+)}$ and $C_{f(-)}$ are the two possible roots and $C_{f(+)} > C_{f(-)}$ provided that

$$g_{m1} > 4g_0 \tag{7}$$

$$C_T > \frac{2g_0}{\omega_0\sqrt{1-\frac{4}{\alpha}}} \tag{8}$$

$$C_{\rm neg} < C_s. \tag{9}$$

III. IM Analysis

In order to carry out the two-tone IM analysis of the active filter, the following assumptions have been made.

1) The filter is operated well below saturation. In this weakly nonlinear case, the Volterra series is valid and only nonlinear transfer function up to the third-order is retained in the formulation.
2) The MESFET is modeled by a simple equivalent circuit in which the controlled drain current source are the only nonlinear element. The drain-to-source current $i_{\rm ds}$ is approximated by
$$i_{\rm ds} = g_{m1}v_{\rm gs} + g_{m2}v_{\rm gs}^2 + g_{m3}v_{\rm gs}^3$$
where g_{m1}, g_{m2} and g_{m3} are bias-dependent coefficients. Note that the nonlinear effect of the gate–source junction capacitance is usually negligibly small, in comparison with the mixing contributions associated with g_{m3} at a low gigahertz frequency range.
3) The generation of high-order mixing products caused by the interactions between the nonlinearities of different FET circuits are neglected here. This is justified by the fact that the first-order mixing products $({\rm dc}, \omega_1 \pm \omega_2, 2\omega_1, 2\omega_2)$ are very small due to the low shunting impedance of the resonator at these frequencies.

As a result, the IM distortion power delivered to the load can be expressed as

$$P_{\rm im}(2\omega_1 - \omega_2) = \frac{1}{2\omega_0 C_b}|j i_{\rm im1} + i_{\rm im2}|^2 \tag{10}$$

where $i_{\rm im1}$ and $i_{\rm im2}$ are the IM distortion currents generated by the individual FET circuit (Fig. 5). By applying the Volterra-series concepts and the method of nonlinear currents [5], the following expressions may be derived:

$$\begin{aligned} i_{\rm im}&(2\omega_1 - \omega_2) \\ &= K_3(2\omega_1 - \omega_2)\left\{2g_{m2}^2 K_2(2\omega_1)\right. \\ &\qquad \left. + 4g_{m2}^2 K_2(\omega_1 - \omega_2) + 3g_{m3}\right\} \\ &\quad \times K_1(\omega_1)^2 K_1(-\omega_2)\frac{V_r^2 V_r^*}{8} \end{aligned} \tag{11}$$

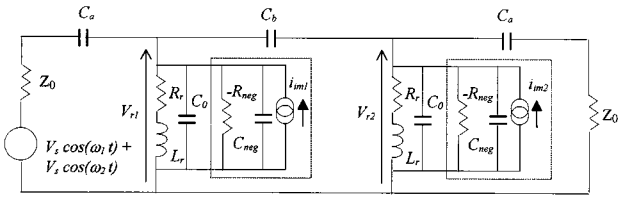

Fig. 5. IM analysis—filter circuit model.

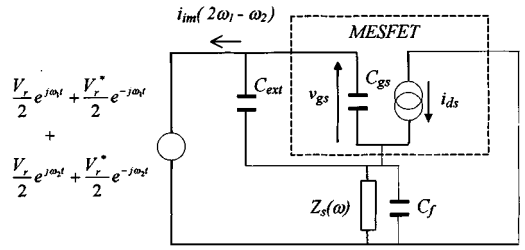

Fig. 6. IM analysis—FET circuit model.

$$K_1(\omega) = \frac{\dfrac{C_f}{C_T}}{1 + \dfrac{C_f}{C_T} + \dfrac{g_{m1}}{j\omega C_T}} \tag{12}$$

$$K_2(\omega) = \frac{-1}{g_{m1} + j\omega C_T + j\omega C_f + Y_s(\omega)} \tag{13}$$

$$K_3(\omega) = \frac{1}{1 + \dfrac{C_f}{C_T} + \dfrac{g_{m1}}{j\omega C_T}} \tag{14}$$

where $i_{\rm im}(2\omega_1 - \omega_2)$ is the IM distortion currents produced by the nonlinear circuit model, shown in Fig. 6. Note that no such information as the phase relationship between the two input signals is required, given the way this problem is formulated. In practice, the third-order mixing term associated g_{m2} is usually less than one-tenth of the term containing g_{m3}. Moreover, as the frequency separation between the two input signals is small ($\omega_1 \approx \omega_2 \approx \omega_0$) and $Z_s(\omega) \approx 0$ at low frequencies. Consequently, (11) may be simplified as

$$i_{\rm im}(2\omega_1 - \omega_2) \approx G V_r^2 V_r^*$$

where

$$G = \frac{3g_{m3}}{8} K_1(\omega_0)^2 K_1(-\omega_0) K_3(\omega_0). \tag{15}$$

Combining (4) and (12)–(15), we obtain

$$G = \frac{3g_{m3}}{8} \frac{\left(1 + \frac{C_f}{C_T} + j\frac{\alpha}{\beta}\right)^2}{\alpha^3}. \tag{16}$$

Consequently, (10) can be rewritten as

$$P_{\rm im}(2\omega_1 - \omega_2) = \frac{1}{2\omega_0 C_b} \left| jV_{r1}^2 V_{r1}^* + V_{r2}^2 V_{r2}^* \right|^2 |G|^2$$

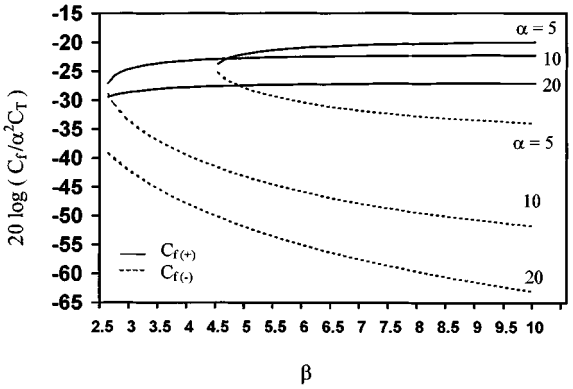

Fig. 7. IM distortion factor as a function of α and β.

where V_{r1} and V_{r2} are the fundamental coefficients of the corresponding voltages across the resonators (Fig. 5). For the narrow-band filter under consideration, it can further be shown that [6]

$$V_{r2} = jV_{r1}$$
$$|V_{r1}|^2 = \frac{|V_s|^2}{4\omega_0 C_b Z_0}$$

hence,

$$\begin{aligned} P_{\rm im}(2\omega_1 - \omega_2) &= \frac{2}{\omega_0 C_b} |G|^2 |V_{r1}|^6 \\ &= \frac{2}{\omega_0 C_b} |G|^2 \frac{|V_s|^6}{(4\omega_0 C_b Z_0)^3} \\ &= \left(\frac{2}{\omega_0 C_b}\right)^4 |G|^2 P_{\rm in}^3 \\ &= 64\omega_0^4 L_r^4 \left(\frac{\omega_0}{\rm BW}\right)^4 \left(\frac{3g_{m3}}{8}\right)^2 \left(\frac{C_f}{\alpha^2 C_T}\right)^2 P_{\rm in}^3 \end{aligned} \tag{17}$$

where BW is the bandwidth of the filter, and $P_{\rm in}$ is the available input power. Furthermore, the third-order intercept point of the filter can be derived as

$$\begin{aligned} {\rm IP3\ (dBm)} = 30 &- 20\log\left(2\sqrt{2}\omega_0 L_r \frac{\omega_0}{\rm BW}\right) \\ &- 20\log\left(\frac{3|g_{m3}|}{8}\right) - 20\log\left(\frac{C_f}{\alpha^2 C_T}\right). \end{aligned} \tag{18}$$

The above expression reveals the influence of device parameters, component values, and filter characteristics on the IM performance of the filter circuit as follows.

1) Fig. 7 shows the plot of $20\ \log(C_f/\alpha^2 C_T)$ as a function of α and β, in combined with (6). It can be seen from the diagram that $C_{f(-)}$ should be chosen for low IM distortion requirements. Furthermore, the IM distortion level decreases with increasing α (g_{m1}) and β (C_T) values.
2) Losses within the passive part of the filter, characterized by the inductor Q-factor, have a direct effect on the IM performance. Equation (17) indicated that IM distortion level decreases with increasing Q-factor (decreasing g_0).
3) The bandwidth of the filter has a strong effect on distortion generation (to the fourth-power), although the internal voltages within a resonator are only scaled in inverse proportion to its bandwidth.

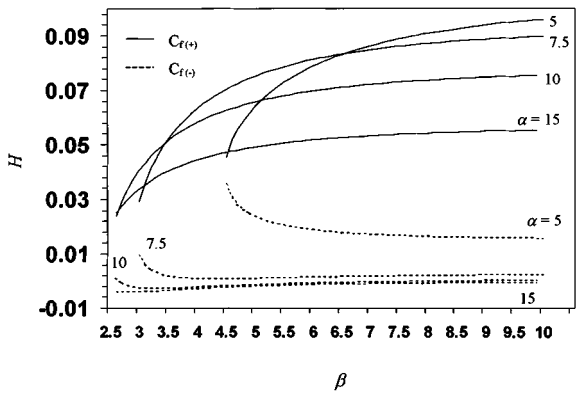

Fig. 8. Variations of H as a function of α and β.

4) g_{m1} and g_{m3} are bias-dependent coefficients, and it might be possible to further reduce distortion by changing the bias condition of the MESFET device.

IV. Gain Compression Analysis

Any transistor is inherently nonlinear and will be driven into saturation as the input power level is increased. Following the same procedure described previously, a formula for the gain compression factor of the active filter can be derived as

$$G.C.\ (\text{dB}) = -20\log\left|1 + G\left(\frac{2}{\omega_0 C_b}\right)^2 P_{\text{in}}\right|. \tag{19}$$

Furthermore, the above expression may be approximated by

$$G.C.\ (\text{dB}) \approx -20\log\left\{1 + 2\,\text{Re}[G]\left(\frac{2}{\omega_0 C_b}\right)^2 P_{\text{in}}\right\} \tag{20}$$

provided that the filter is operated below the 1-dB gain compression point. The above expression can be reduced to

$$G.C.\ (\text{dB}) \approx -20\log\left\{1 + \frac{3g_{m3}}{4}\left(\frac{2}{\omega_0 C_b}\right)^2 H P_{\text{in}}\right\} \tag{21}$$

where

$$H = \frac{\left(1 + \frac{C_f}{C_T}\right)^2 - \frac{\alpha^2}{\beta^2}}{\alpha^3}. \tag{22}$$

The variations of H as a function of α and β has been evaluated and plotted in Fig. 8. Note that, in practice, the sign of g_{m3} is usually negative, which causes gain compression at low input power level. It can be observed from the diagram that the power saturation effect is strong if $C_{f(+)}$ is used in the calculations. In addition, when $C_{f(-)}$ is assumed and $\propto > 7.5$, the term in (21) containing H is small and almost independent of the value of β (C_T).

V. Experiments and Discussions

In order to verify the validity of the above theory, single- and two-tone measurements were performed on an experimental filter constructed using lumped components. The negative-resistance circuits employed here consist of Siemens CFY 30 GaAs MESFET's and chip capacitors connected between the gate and source terminals. The test setup for the measurement comprises

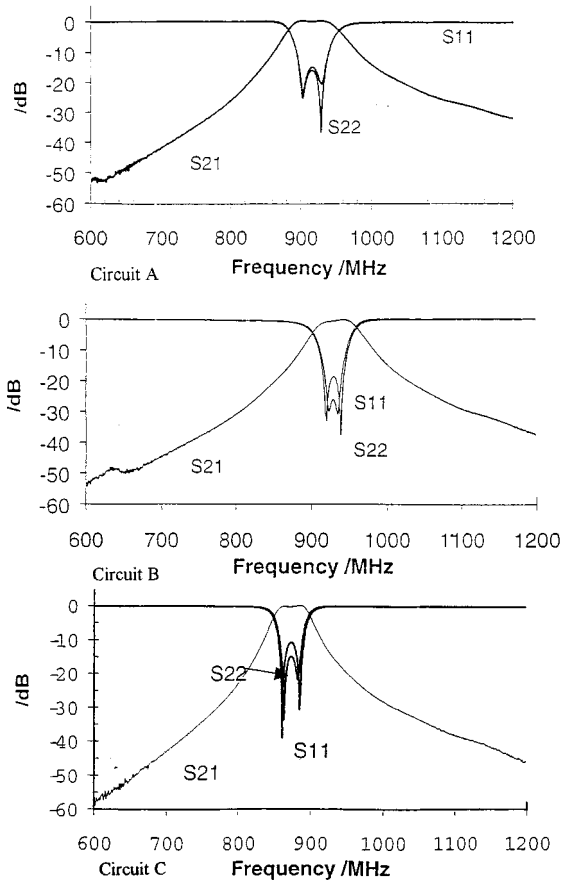

Fig. 9. Measured frequency responses of experimental active filters.

two synthesized frequency sources offset by 5 MHz close to the center of the filter passband. IM products generated by the system was checked to be negligibly small relative to those produced by the filter circuit. Without compensation, the passive design was found to have an insertion loss of about 9 dB, with a center frequency of around 900 MHz. The value of g_0 is estimated to be approximately 3 mS. Fig. 9 shows the measured frequency response of the three fabricated filter circuits with a device drain current I_{ds} of 4 mA ($g_{m1} \approx 25$ mS and, hence, $\alpha \approx 8$). The design parameters of these filters are given below.

Circuit A:

$$C_{\text{ext}} = 2\ \text{pF}(\beta \approx 4.5), \qquad \text{with } C_f = C_{f(+)} = 10\ \text{pF}.$$

Circuit B:

$$C_{\text{ext}} = 2\ \text{pF}(\beta \approx 4.5), \qquad \text{with } C_f = C_{f(-)} = 1.5\ \text{pF}.$$

Circuit C:

$$C_{\text{ext}} = 4\ \text{pF}(\beta \approx 9), \qquad \text{with } C_f = C_{f(-)} = 1\ \text{pF}.$$

All measurements were performed at the same bias conditions (I_{ds} and V_{ds}), thus keeping the values of g_{m1} and g_{m3} unchanged. Gain compression and two-tone IM measurements were conducted for various input power levels ranging from –18 to 8 dBm, and the results are given in Figs. 10 and 11. The measured IM performances of Circuits A and B indicated that a significant improvement (>20 dB) can be attained by properly choosing the value of the feedback capacitor. A further reduction of the IM distortion level (about 10-dB improvement) has

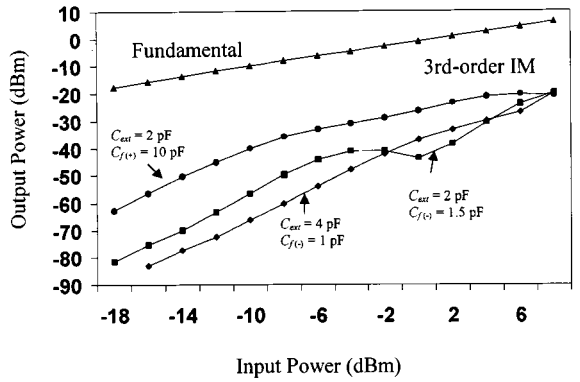

Fig. 10. Measured third-order IM distortion performances of experimental active filters.

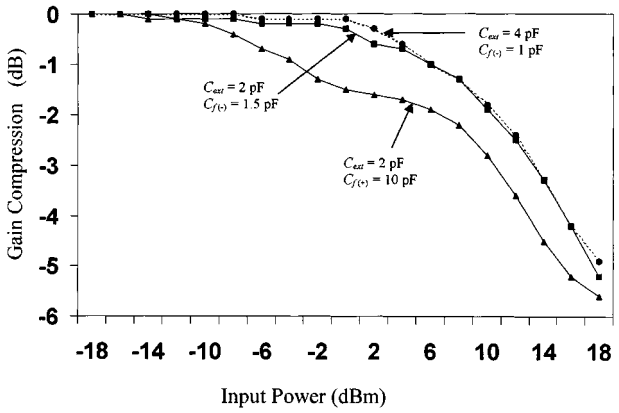

Fig. 11. Measured gain compression performances of experimental active filters.

also been demonstrated by using a larger value of C_{ext} (Circuit C). Moreover, the power measurements has also shown an increase in input power requirements at a 1-dB compression point for filter Circuits B and C.

VI. Conclusion

A new technique to reduce the in-band third-order IM distortion in active bandpass filters using negative-resistance circuits is presented. A simple expression relating the IM distortion to circuit and device parameters has been formulated based upon the Volterra series method. Experimental results confirmed that the third-order IM distortion is strongly dependent on the values of the feedback capacitors and the external gate-to-source capacitor. The formulas also suggested that a further reduction of the IM distortion may be attained in these filters by employing an MESFET of large transconductance value and inductors of a high Q-factor. The method of analysis described here can easily be extended to the design of higher order active filters.

Appendix

This Appendix provides the design equations for the second-order Butterworth bandpass filter shown in Fig. 1. Under the narrow-band assumption, the component values can be calculated by [6]

$$\omega_0 C_r = \frac{1}{\omega_0 L_r} \tag{A1}$$

$$\omega_0 C_b = \frac{1}{1.414\omega_0 L_r}\left(\frac{\omega_U - \omega_L}{\omega_0}\right) \tag{A2}$$

$$\omega_0 C_a Z_0 = \sqrt{\frac{\omega_0 C_b Z_0}{1 - \omega_0 C_b Z_0}} \tag{A3}$$

$$C_s = C_r - C_b - \frac{C_a}{1 + (\omega_0 C_a Z_0)^2} \tag{A4}$$

where ω_L, ω_U, and ω_0 are the lower cutoff, upper cutoff , and center frequencies (radian per second) of the passband characteristics, respectively.

References

[1] U. Karacaoglu and I. D. Robertson, "MMIC active bandpass filters using varactor-tuned negative resistance elements," *IEEE Trans. Microwave Theory Tech.*, vol. 43, pp. 2926–2932, Dec. 1995.

[2] B. P. Hopf, I. Wolff, and M. Guglielmi, "Coplanar MMIC active bandpass filters using negative resistance circuits," *IEEE Trans. Microwave Theory Tech.*, vol. 42, pp. 2598–2602, Dec. 1994.

[3] V. Aparin and P. Katzin, "Active GaAs MMIC bandpass filters with automatic frequency tuning and insertion loss control," *IEEE J. Solid-State Circuits*, vol. 30, pp. 1068–1073, Oct. 1995.

[4] I. C. Hunter and S. R. Chandler, "Intermodulation distortion in active microwave filters," *Proc. Inst. Elect. Eng.*, vol. 145, no. 1, pp. 7–12, Feb. 1998.

[5] J. Bussgang, L. Ehrman, and J. Craham, "Analysis of nonlinear systems with multiple inputs," *Proc. IEEE*, vol. 62, pp. 1089–1119, Aug. 1974.

[6] G. L. Matthaei, L. Young, and E. M. T. Jones, *Microwave Filter Impedance Matching Networks and Coupling Structures*. New York: McGraw-Hill, 1964.

Kwok-Keung M. Cheng (S'90–M'91) received the B.Sc. (first-class honors) degree in electronic engineering and the Ph.D. degree from King's College, University of London, London, U.K., in 1987 and 1993, respectively.

From 1990 to 1992, he was a Research Assistant at King's College, where he was involved in the area of hybrid circuit and MMIC design. From 1993 to 1995, he was a Post-Doctoral Research Associate at King's College, where he was involved with the investigation of coplanar structures for microwave/millimeter-wave applications. In 1996, he was appointed Assistant Professor in the Department of Electronic Engineering at the Chinese University of Hong Kong, Shatin, Hong Kong. He has authored or co-authored over 30 papers in international journals and conferences. He is also a contributing author *MMIC Design* (London, U.K.: IEE, 1995). His current research interests are concerned with the design of MMIC's, oscillators, active filters, and power amplifiers.

Dr. Cheng was the recipient of the 1986 Siemens Prize, the 1987 Institution of Electrical Engineers (IEE) Prize, and the 1988 Convocation Sesquicentennial Prize in Engineering presented by the University of London.

Siu-Chung Chan was born in Hong Kong. He received the B.Eng. and M.Phil. degrees in electronic engineering from the Chinese University of Hong Kong, Shatin, Hong Kong, in 1996 and 1998, respectively.

His current research interests are in the area of MMIC active filter design and wireless communications.